Current Alzheimer Research, 2020, *17*, 69-79

RESEARCH ARTICLE

Disrupted Time-Dependent and Functional Connectivity Brain Network in Alzheimer's Disease: A Resting-State fMRI Study Based on Visibility Graph

Zhongke Gao[1,*], Yanhua Feng[1], Chao Ma[1,*], Kai Ma[2], Qing Cai[1] and for the Alzheimer's Disease Neuroimaging Initiative[#]

[1]*School of Electrical and Information Engineering, Tianjin University, Tianjin, China;* [2]*Principal Researcher at Tencent, Guangdong, China*

ARTICLE HISTORY

Received: August 24, 2019
Revised: November 16, 2019
Accepted: January 20, 2020

DOI:
10.2174/1567205017666200213100607

Abstract: ***Background*:** Alzheimer's Disease (AD) is a progressive neurodegenerative disease with insidious onset, which is difficult to be reversed and cured. Therefore, discovering more precise biological information from neuroimaging biomarkers is crucial for accurate and automatic detection of AD.

***Methods*:** We innovatively used a Visibility Graph (VG) to construct the time-dependent brain networks as well as functional connectivity network to investigate the underlying dynamics of AD brain based on functional magnetic resonance imaging. There were 32 AD patients and 29 Normal Controls (NCs) from the Alzheimer's Disease Neuroimaging Initiative (ADNI) database. First, the VG method mapped the time series of single brain region into networks. By extracting topological properties of the networks, the most significant features were selected as discriminant features into a supporting vector machine for classification. Furthermore, in order to detect abnormalities of these brain regions in the whole AD brain, functional connectivity among different brain regions was calculated based on the correlation of regional degree sequences.

***Results*:** According to the topology abnormalities exploration of local complex networks, we found several abnormal brain regions, including left insular, right posterior cingulate gyrus and other cortical regions. The accuracy of characteristics of the brain regions extracted from local complex networks was 88.52%. Association analysis demonstrated that the left inferior opercular part of frontal gyrus**,** right middle occipital gyrus, right superior parietal gyrus and right precuneus played a tremendous role in AD.

***Conclusion*:** These results would be helpful in revealing the underlying pathological mechanism of the disease.

Keywords: Alzheimer's disease, fMRI, visibility graph, functional networks, classification study, local complex network.

1. INTRODUCTION

Alzheimer's Disease (AD) is a neurodegenerative disease whose etiological factors and pathogenesis are complicated and hard to be clarified completely [1]. Most of the patients are over 65 years old and most of them with cognitive and functional symptoms, including memory disorder, aphasia, agnosia, visual-spatial skills impairment, executive dysfunction, personality and behavioral changes [2-4]. As the pathological factors like amyloid plaque and phosphorylated tau protein often accumulate for a few years before obvious clinical symptoms [5-7], therefore, early diagnosis of patients with Alzheimer's disease is of great significance for their treatment since there is no approved diagnosis or cure for AD. In the past few decades, many researchers have contributed a lot to the pathogenesis and diagnosis of AD from the perspective of functional connectivity, but our understanding of the progression of AD is still rudimentary [8, 9].

Recently, fMRI has been widely used in the diagnosis of AD and the detection of brain dysfunction due to its safety and non-invasiveness, high spatial resolution and repeatability of experimental conditions [10]. The low-frequency fluctuations of Blood Oxygenation Level-Dependent (BOLD) signal in the resting-state reflect the information of neurons and synapses activity in the brain area, the correlation of resting-state time series among multiple brain regions revealing the correlation and communication between the sponta-

*Address correspondence to this author at the School of Electrical and Information Engineering, Tianjin University, Tianjin, China; Tel/Fax: ++86 18612528205, +86(022)27510556; E-mail: chao.ma@tju.edu.cn

[#]*Data used in preparation for this article were obtained from the Alzheimer's Disease Neuroimaging Initiative (ADNI) database (http://adni.loni.usc.edu). As such, the investigators within the ADNI contributed to the design and implementation of ADNI and/or provided data but did not participate in analysis or writing of this report. A complete listing of ADNI investigators can be found at: http://adni.loni.usc.edu/wp-content/uploads/how_to_apply/ADNI_Acknowledgement_List.pdf*

neous neuronal activation patterns of these regions [11]. There are many studies on the establishment of brain networks based on fMRI to reveal the topological structure of AD [12-14]. Studies of functional and structural brain networks have confirmed the irreversible loss of small-world properties and the reduction of network complexity in AD patients [15-17]. Ma *et al.* showed that genes impair cognitive performance of the elderly through the brain functional network [18]. Wang *et al.* reported a disruption of functional connectivity between the hippocampus and several regions such as the medial prefrontal cortex and the posterior cingulate cortex in AD [19]. Event-related fMRI studies have shown that posterior cingulate gyrus, retrosplenial and lateral parietal cortex are active during successful memory recovery in young adults [20]. In addition, using cerebral functional network features can effectively distinguish AD from normal people [21].

The development of complex network theory has attracted the interest of researchers and has been widely used. A review on the complex network analysis of time series is given [22]. The study of the human brain is an important field of complex network applications, for example, using a complex network to study the impact of fatigue state on the accuracy of steady-state visual evoked potential classification [23] and effectively improve the accuracy of fatigue driving state detection [24]. Visibility Graph (VG) was proposed by Lacasa and Luque [25], and it has been widely used in the construction of complex networks. As an effective means of describing time series, VG has the advantages of easy implementation and high computational efficiency, so it has been widely used in the physiological signal analysis in recent years [26, 27]. Previously, VG has been used to construct the complex network of EEG signals for epilepsy patients by combining adaptive optimal kernel time-frequency representation. Its topological features showed significant differences [28]. The Multiplex Limited Penetrable Horizontal Visibility Graph method has been proven to effectively detect fatigue driving and explore the fatigue behavior of the brain [29], and also has been used in EEG signal studies of AD [30]. This fully demonstrated that VG is a powerful tool for network construction and a promising method for studying fMRI image data of AD. By using the graph-theoretical approaches of a complex network to study AD is a new perspective and it effectively discovered important time-dependent non-linear information contained in physiological signals [31].

Although there are many studies on abnormal functional connections between brain regions of AD based on fMRI [32], it is unclear whether the abnormalities of the AD brain could be detected by both local network of specific brain and whole-brain functional network. In the present study, we employed resting-state fMRI (rs-fMRI) data to investigate single regional time series based on VG complex network analysis and constructed functional brain network from degree sequences. The nonlinear characteristics of AD were analyzed from both the single time series and whole-brain functional network. There are two main purposes: 1. To illustrate the pathological regions of AD in terms of temporal characteristics. 2. Find sensitive biomarkers, which could be helpful for automated diagnosis of the disease.

2. MATERIALS AND METHODS

2.1. Subjects

The data used in this study was derived from the Alzheimer's Disease Neuroimaging Initiative (ADNI) database, which collects a variety of neuroimaging data, including MRI and PET images, genetics, cognitive tests, cerebrospinal fluid and blood biomarkers for early detection and tracking of AD. ADNI is committed to advancing AD research by enabling researchers around the world to share data to support the advancement of AD intervention, prevention and treatment. We selected 32 patients with Alzheimer's disease (average age 75.4 years, 17 male) and 29 age-matched controls normal (average age 74.5 years, 15 male). Data for this study were selected based on the availability of resting-state fMRI datasets for age-matched healthy normal subjects and patients with AD. The patients with AD had a Mini-Mental State Examination (MMSE) score of 14-26 and a Clinical Dementia Rating (CDR) of 0.5 or 1.0 and met the National Institute of Neurological and Communicative Disorders and Stroke and the Alzheimer's Disease and Related Disorders Association (NINCDS/ADRDA) criteria for probable AD. The normal subjects were non-depressed, non-MCI, and non-demented and had a MMSE score of 27-30 and a CDR of 0. For more experimental details, please refer to http://adni.loni.usc.edu/. Demographics and clinical information are described in Table **1**.

2.2. Data Preprocessing

Resting-state fMRI data scans were acquired with 3.0T Philips Medical Systems scanners. Acquisitions were performed according to the ADNI acquisition protocol. All fMRI data were preprocessed using SPM8 (http://www.fil.ion.ucl.ac.uk/spm/software/spm8/): the data were realigned and normalized to a standard template and resampled to 3×3×3mm voxels. All fMRI time-series under-

Table 1. Demographic and clinical characteristics of AD patients and control subjects. second and third columns present group characteristics (Mean ± Standard Deviation). Fourth column and fifth column present T-values and *p*-values for statistical significance of between-group differences.

-	ADs	Controls	t	p
Female/Male	15/17	14/15	-	-
Age	75.41±4.20	74.52±4.32	0.814	0.419
MMSE	20.25±3.33	29.35±0.81	-14.310	7.60e-21
CDR	0.953±0.35	0.035±0.13	13.518	1.01e-19

went band-pass temporal filtering (0.01-0.08Hz), nuisance signal removal from ventricles, deep white matter, global mean signal removal, and 6-parameter rigid-body motion correction. The raw resting-state fMRI data have 140 time points and the first 5 time points were removed because of potential nonequilibrium effects of magnetization. 90 regional time series were extracted by averaging voxel time series within each anatomically defined region using the Automated-Anatomical-Labeling (AAL) template.

2.3. From Time Series to Complex Network

The visibility graph is a complex network construction method for one-dimensional time series, which can preserve the time characteristics of the series [25, 33]. For time series $x_t = \{x_i\}; i = 1, \ldots, N$, we can map it to a VG in the following manner. As shown in Fig. (**1**), Fig. (**1.a**) shows eight points in the time series x_t, the vertical black bars represent the amplitude of the time series, and each data point (black dot) is regarded as a node of the complex network. If the straight line between two nodes does not intersect the bars of other intermediate nodes, there is a connection between the two nodes and Fig. (**1.b**). shows the corresponding VG map and a_i, corresponds to the *i*th point of the time series, x_i. Two nodes of the graph, a_m and a_n, are connected *via* a bidirectional edge if and only if:

$$x_{m+j} < x_n + \left(\frac{n-(m+j)}{n-m}\right)(x_m - x_n) \quad \forall j \in Z^+; j < n-m$$

Thus, each adjacency matrix is composed of 1 or 0, respectively, indicating the corresponding nodes are connected or not. We mapped the time series of each brain region into the VG network, so we got 90 binary adjacency matrices for each subject. The statistical feature of local complex networks was analyzed to locate brain regions with abnormal temporal characteristics caused by AD from the perspective of a single brain region.

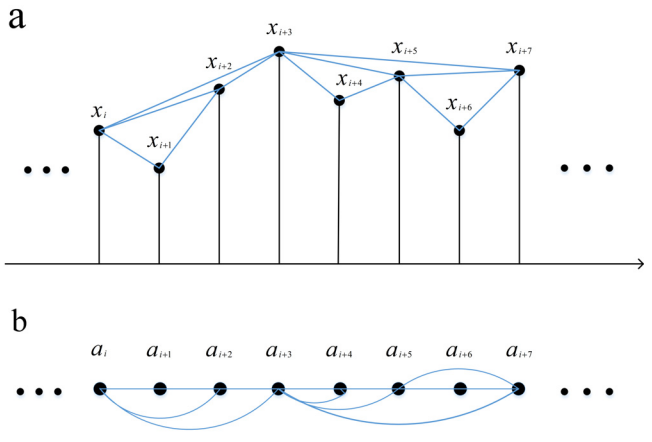

Fig. (1). Illustrating the process of mapping one-dimensional time series (Fig. **1a**) to VG (Fig. **1b**). Each blue line in Fig. **1a** shows the two connected points that can see each other. *(A higher resolution / colour version of this figure is available in the electronic copy of the article).*

2.4. Functional Brain Network

The complex network constructed by VG is based on a single time series and cannot convey similar or synchronous information between series. In order to study the effect of local brain abnormalities on the whole brain system, we constructed a functional connectivity network based on the whole brain. In this part, the functional brain network is constructed by the method of degree sequence correlation to study the effect of Alzheimer's disease on the topological structure of the brain network. After the complex network of each brain region is obtained by the above VG method, the degree sequence is obtained, then the Pearson correlation of the degree sequence among brain regions obtained a 90×90 weighted adjacency matrix.

Finally, we applied fisher's r-to-z transformation on the elements of the Pearson correlation matrix to improve the normality of the correlation coefficients, as follows:

$$z = \frac{1}{2}\left[\ln(1+r) - \ln(1-r)\right]$$

where r is the Pearson correlation coefficient and z is approximately a normal distribution with standard deviation $\sigma_z = 1/\sqrt{N-3}$. The brain networks are represented in the form of z-maps. The threshold is set to 0.3, which is defined as the ratio of the number of existing edges to the maximum possible edge number in the network.

2.5. Network Metrics

In order to analyze the statistical feature of networks, we calculated the degree, betweenness centrality, local efficiency, global clustering coefficient of local complex networks and weighted degree of the functional brain network.

2.5.1. Degree

The degree is a common measure of node centrality, which reflects the importance of nodes in the network. The degree of an individual node in the network is equal to the number of links connected to that node [34]. For binary adjacency matrix, the degree of node i:

$$k_i = \sum_{j \in N} a_{ij}$$

For weighted degree of i:

$$k_i^w = \sum_{j \in N} w_{ij}$$

where N is the set of all nodes in the network and (i, j) is a link between nodes i and j, ($i, j \in N$). a_{ij} is the connection status between i and j: $a_{ij} = 1$ when link (i, j) exists (when i and j are neighbors); $a_{ij} = 0$ otherwise ($a_{ii} = 0$ for all i) and w_{ij} is the weighted value of connection status between i and j.

2.5.2. Betweenness Centrality

Unlike the degree centrality, betweenness centrality is a more global and sensitive measure, defined as the fraction of all shortest paths in the network that pass through a given node [35]:

$$b_i = \frac{1}{(n-1)(n-2)} \sum_{\substack{h,j \in N \\ h \neq j, h \neq i, j \neq i}} \frac{\rho_{hj}(i)}{\rho_{hj}}$$

where ρ_{hj} is the number of shortest paths between h and j, and $\rho_{hj}(i)$ is the number of shortest paths between h and j that pass through i.

2.5.3. Local Efficiency

Local efficiency measures the aggregation degree of the sub-network formed by the neighbor nodes connected with node k [36]:

$$E_{local}(k) = \frac{1}{N_{G_k}\left(N_{G_k}-1\right)} \sum_{i \neq j \in G_k} \frac{1}{d_{ij}}$$

where G_k represents the sub-network constituted by the neighbor nodes of node k, and N_{G_k} is the number of the nodes in the network G_k.

2.5.4. Global Clustering Coefficient

The global clustering coefficient (Glob Cp) evaluates the overall level of clusters in the network [37], and the calculation formula is as follows:

$$C = \frac{\tau_{\Delta}}{\tau}$$

where τ_{Δ} represents the number of closed triplets in a VG network and a closed triplet is composed of three triplets. τ represents the number of triplets (*i.e.,* three nodes connected by two ties) in a VG network.

2.6. Classification Method

We choose the support vector machine (SVM) classifier, which is widely used in pattern recognition in various fields [38]. It has advantages in solving nonlinearity, small sample, high dimension and local extremum problems. The main ideas of SVM are to nonlinearly map data to a high-dimensional feature space and construct the optimal hyperplane [39]. For a detailed understanding of the principle of SVM, one can refer to the literature [40, 41].

In this study, We applied LIBSVM library [42] on MATLAB and set the kernel function as "linear kernel (default)". Based on the features extracted from local brain networks, linear kernel function combined with leave-one-out cross validation method showed good classification performance.

2.7. Statistical Analyses

One-way Analysis of Variance (ANOVA) was performed to examine differences between the AD patients and Controls Normal (CNs) and the region of $p < 0.05$ was selected for statistical analysis. For demographic factors, we put participant's age, sex and education (years) as covariates into the ANCOVA model when comparing the group differences of network parameters.

In order to explore the effects of abnormal brain regions obtained from single-region time series analysis on the whole-brain functional connectivity network, we constructed an effective functional connectivity network, which obtains the degree sequences of different regions from the local complex network of single-region series, and then calculated Pearson correlation between the two-degree sequences of every two brain regions to obtain a 90×90 weighted adjacency matrix. We used one-way ANOVA to analyze the topological characteristics of the network, i.e. weighted degree, to find out the brain regions with significant differences between the AD group and the control group. Next, we selected the brain regions with abnormal characteristics of both local complex network and functional network. For each of these brain regions, we did the Pearson correlation between the topological characteristics of its local complex network of single-region series and the degree of its functional network to explore the impact of changes in the single brain region series on the connectivity of the functional network.

3. RESULTS

3.1. Network of the Local Brain Region

VG has been used to build complex networks to analyze EEG signals in patients with AD [43], but it has not yet been applied to fMRI signal analysis. Therefore, to explore the local complex network topology abnormalities of Alzheimer's single region fMRI series is of great significance for revealing its structure and topological characteristics. For the adjacency matrix of each brain region, we extracted the topological characteristics of an average of nodes Degree value (Deg), an average of nodes Betweenness centrality (Be), average Local Efficiency (LocE), and global clustering coefficient (Glob Cp). We used one-way ANOVA to identify significant differences in temporal characteristics between AD patients and CNs. We identified that the topological characteristic of 17 brain regions showed significant discrimination between the AD patients and the control group, with p values less than 0.05. These brain regions include left superior orbital frontal gyrus (ORBsup.L), right superior orbital frontal gyrus (ORBsup.R), left inferior opercular part of frontal gyrus (IFGoperc.L), right inferior triangle frontal gyrus (IFGtriang.R), right inferior orbital frontal gyrus (ORBinf.R), left superior medial orbital frontal gyrus (ORBsupmed.L), left insular (INS.L), right posterior cingulate gyrus and its lateral circumferential gyrus (PCG.R), left cuneus (CUN.L), right lingual gyrus (LING.R), left superior occipital gyrus (SOG.L), right superior occipital gyrus (SOG.R), right middle occipital gyrus (MOG.R), right superior parietal gyrus (SPG.R), right precuneus (PCUN.R), Heschl's left gyrus (HES.L) and right middle temporal gyrus (MTG.R).

Fig. (**2**) and Table **2** illustrate group differences of the network of local brain region on the topological characteristic indexes. For these selected regions, most of them have been proved to be pathologically related to AD, but there are also a few undetected regions, which make a great contribution to revealing the mechanism of AD. As presented in Table **2**, we listed the brain regions with statistical value $p < 0.05$, most regions of AD group display increased Deg and decreased LocE; for the average local efficiency and Global clustering coefficient, the mean values of the AD group generally decreased compared to CNs.

3.2. Classification

Based on the selected features above, the SVM classifier and the method of leave-one-out cross validation were ap-

Table 2. Characteristics of the brain regions that were significantly different between the two groups.

Network Measures	Brain Region	CN	AD	F	p
Deg	ORBsup.L	7.106(±0.414)	6.863(±0.439)	5.441	0.023
	ORBsup.R	7.093(±0.416)	6.851(±0.451)	4.403	0.040
	PCG.R	6.765(±0.464)	7.033(±0.450)	4.055	0.049
	CUN.L	6.827(±0.417)	7.144(±0.493)	6.658	0.013
	LING.R	6.829(±0.532)	7.115(±0.476)	4.446	0.039
	SOG.R	6.955(±0.503)	7.261(±0.533)	4.275	0.043
	MOG.R	6.922(±0.538)	7.208(±0.470)	4.561	0.037
Be	IFGoperc.L	337.392(±27.345)	354.252(±28.861)	4.632	0.036
	IFGtriang.R	359.103(±35.039)	338.091(±29.268)	7.905	0.007
LocE	ORBinf.R	0.857±(0.008)	0.852(±0.010)	4.380	0.041
	SOG.L	0.857(±0.008)	0.852(±0.010)	4.109	0.047
	SPG.R	0.859(±0.006)	0.853(±0.009)	6.646	0.013
	PCUN.R	0.857(±0.008)	0.851(±0.009)	6.993	0.011
	MTG.R	0.856(±0.008)	0.851(±0.010)	4.442	0.039
Glob Cp	ORBsupmed.L	0.516(±0.024)	0.503(±0.023)	4.382	0.041
	INS.L	0.509(±0.025)	0.493(±0.026)	5.727	0.020
	SOG.L	0.511(±0.029)	0.528(±0.034)	4.204	0.045
	HES.L	0.499(±0.025)	0.485(±0.028)	4.376	0.041

The characteristics of the brain regions extracted from local complex networks. The values are represented with a mean (standard deviation) of each group. Deg: degree; Be: betweenness centrality; LocE: local efficiency; Glob Cp: global clustering coefficient. Among them, Deg, Be, LocE take the average value of local complex network.

Table 3. Classification accuracy obtained by using leave-one-out cross validation method.

Network Measures Used in the SVM Model	ACC%	Network Measures Used in the SVM Model	ACC%
Deg	67.21	Be + Glob Cp	78.69
Be	63.93	LocE + Glob Cp	60.66
LocE	63.93	Deg + Be + LocE	80.33
Glob Cp	67.21	Deg + Be + Glob Cp	73.77
Deg + Be	67.21	Deg + LocE + Glob Cp	80.33
Deg + LocE	75.41	Be + LocE + Glob Cp	80.33
Deg + Glob Cp	70.49	Deg + Be + LocE + Glob Cp	88.52
Be + LocE	75.41		

Deg: degree; Be: betweenness centrality; LocE: local efficiency; Glob Cp: global clustering coefficient. Among them, Deg, Be, LocE take the average value of local complex network.

plied to obtain the classification accuracy. As shown in Table **3**, the classifier was trained by Deg, Be, LocE and Glob Cp respectively or their combination. Among them, the combination of these four attributes had the highest classification accuracy, which is 88.52%. This indicated that VG is a potential method to diagnose AD. Additionally, the graph theory is used to study the human brain's network to discover the differences caused by AD, thus promoting the development of AD diagnostic technology.

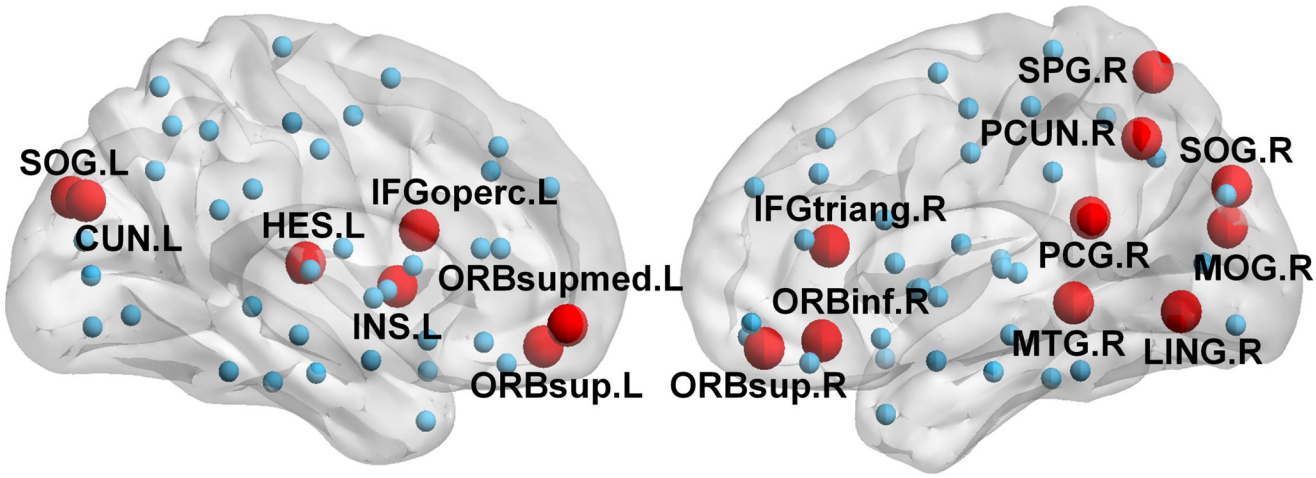

Fig. (2). The brain distribution map of abnormal brain regions we selected from local complex networks (the red part is the abnormal brain region). *(A higher resolution / colour version of this figure is available in the electronic copy of the article).*

3.3. Local Brain Abnormalities Effects on Global Network Measures

In this part, we employed weighted degree values to explore dynamic behavior based on network analysis. Degree centrality is the most direct measure to characterize the centrality of nodes in graph theory and network analysis. The greater the degree of a node, the more important it is in the network. In order to quantify the group differences of the functional network between AD patients and CNs, we used one-way ANOVA to analyze the topological characteristics of networks, i.e. weighted degree. For different brain regions, the *p*-values less than 0.05 indicate statistical difference. Significant differences could be observed in IFGoperc.L, SOG.R, MOG.R, SPG.R and PCUN.R between the AD group and the control group. Simultaneously, these brain regions also showed significant differences in the topological structure of the local complex network of a single brain region. As shown in Fig. (**3**), compared with the control group, the degree of these brain regions in AD patients decreased significantly.

As shown in Fig. (**4**), finally, IFGoperc.L, MOG.R, PCUN.R and SPG.R were found to have a significant correlation between the topological characteristics of local complex networks and the degree of functional networks. It can be seen that their self-generated changes play an important role in the connectivity changes of the whole functional network. Therefore, we considered that the changes in these four brain regions are one of the main causes of AD pathology. Most of these brain regions are located in the right hemisphere.

4. DISCUSSION

In this paper, we constructed the local complex network of single-region series and the functional connectivity network of the whole brain with the method of visibility graph to study the topology abnormalities of AD patients. For the local complex network from single regions, we found that there were significant differences in the network characteristics of some local regions. Considering the difference of local complex network, disrupted connections across different brain regions would probably be the main cause of Alzheimer's disease. Therefore, we constructed the whole-brain functional network from the degree sequence of the local complex network. The results showed that IFGoperc.L, SOG.R, MOG.R, SPG.R and PCUN.R were also involved in the connection changes and impairments of nerve cells among brain regions. Correlation analyses showed that single region abnormality was correlated with interregional connectivity disruptions.

For local complex network of specific fMRI series, we found that brain damage mainly occurred in the inferior frontal gyrus, occipital lobe and temporal lobe. The local complex network topological characteristics of these brain regions can effectively distinguish AD from CNs. Among these selected regions, the insula is of particular interest because it performed a critical role in conscious emotional feelings, cognitive and sensory processing [44, 45]. Amyloid-β ($A\beta$) plaques, neurofibrillary tangles and significant volume atrophy, might be the cause of the insula dysfunction in AD patients [46-49]. Previous studies revealed that the impaired functional network of abnormal insula increases the risk of AD and plays an important role in the pathological changes in the early stages of AD [50]. The functional connectivity networks in AD patients are significantly reduced in the left insula compared with those in CNs due to cholinergic dysfunction in AD [51-53]. Previous studies have suggested that the posterior cingulate cortex has memory-related and "evaluative" functions [54], which is one of the core areas of AD progression [55, 56]. The regional functional alterations such as Heschl's left gyrus, right middle temporal gyrus, right superior parietal gyrus and right posterior cingulate gyrus, which we identified, are also found to be effectively detect AD patients from the CNs [57, 58]. In AD, the deposition of $A\beta$ proteins caused by the course of the disease is highly correlated with the default pattern network in adults [20]. The active regions of the default mode network include frontal regions along the midline, posterior cingulate, retrosplenial cortex, precuneus, medial and lateral posterior parietal regions [59, 60], simultaneously, medial temporal lobe is also active in the default mode network [61]. Compared with our findings, most of the brain regions we identified belonged to the default mode network. Furthermore, greater

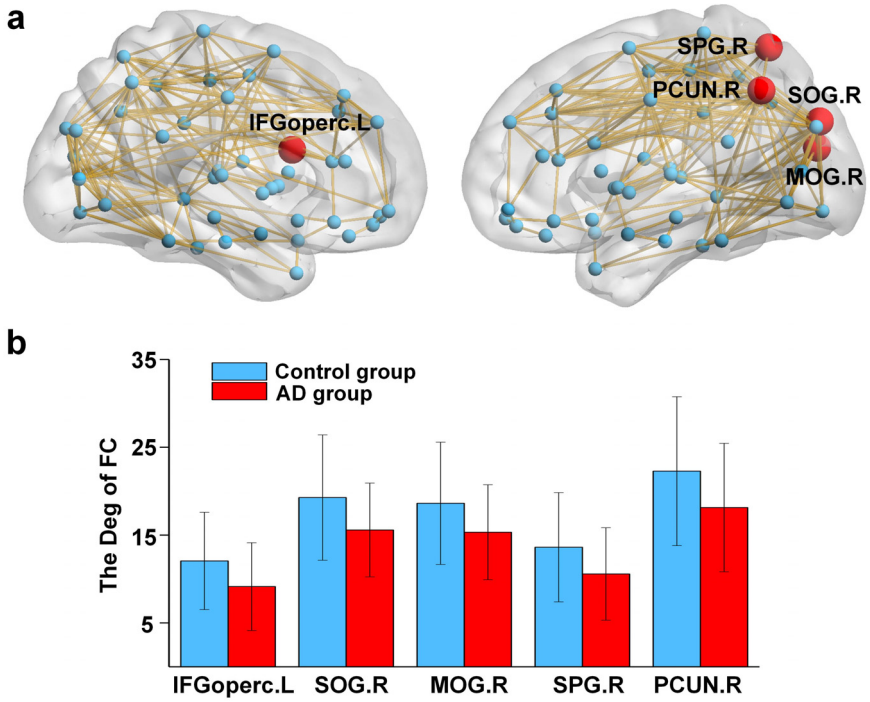

Fig. (3). The weighted degree of IFGoperc.L, SOG.R, MOG.R, SPG.R and PCUN.R in the whole brain connectivity network were significantly different ($p<0.05$) between the AD group and the control group. **(a)** The distribution of brain regions with a decreased nodal degree in the AD group. **(b)** The histogram of IFGoperc.L, SOG.R, MOG.R, SPG.R and PCUN.R in the functional connectivity (FC). *(A higher resolution / colour version of this figure is available in the electronic copy of the article).*

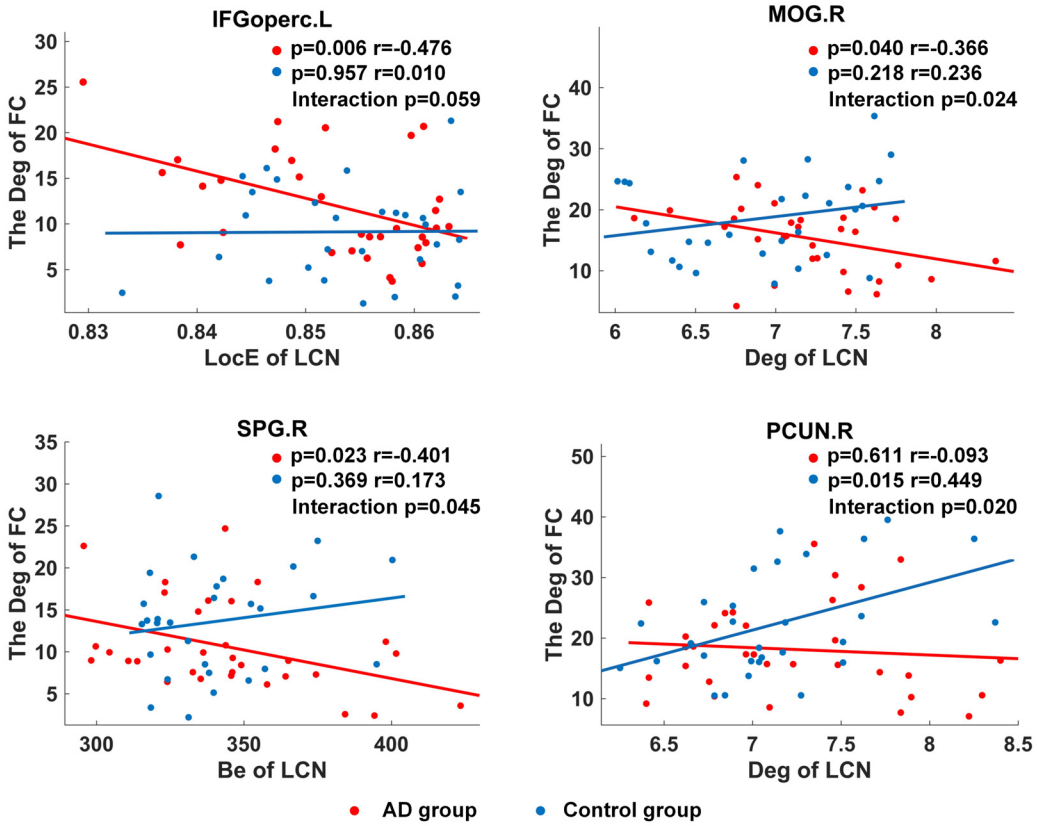

Fig. (4). The correlation between the weighted degree of Functional Connectivity (FC) network and topological features of local complex network (LCN) for IFGoperc.L (left inferior opercular part of frontal gyrus), MOG.R (right middle occipital gyrus), SPG.R (right superior parietal gyrus) and PCUN.R (right precuneus). LocE: average local efficiency; Deg: average of nodes degree value; Be: average of nodes betweenness centrality. *(A higher resolution / colour version of this figure is available in the electronic copy of the article).*

deposition of $A\beta$ was observed in the lingual gyri and its complexity on multiple time scales was reduced [11, 62].

Current results showed that functional connectivity brain networks of Alzheimer's patients are significantly decreased in SOG.R and MOG.R, which is consistent with previous findings [63, 64]. The neuropathology of the occipital lobe is related to the development of visual hallucinations in AD, and visual hallucinations are significantly associated with the morbidity of AD [65]. Moreover, the occipital lobe complexity of AD patients has been shown to be significantly reduced [66]. Another important abnormal hub region we found was the precuneus. The precuneus occupies an important position in connectivity abnormalities of brain network in Alzheimer's disease [67]. GM loss was observed in the posterior cingulate gyrus and precuneus in AD patients [68]. Recent functional neuroimaging studies have demonstrated that the precuneus is involved in the progression of AD, which is related to cognitive functions such as episodic memory retrieval and self-processing operations [69].

To our knowledge, this is the first study combining a single brain region network with a functional network based on fMRI data. Researchers considered AD as a disconnection syndrome [70], in which local regional dysfunction may spread through neurons in the functional proximity of specific brain regions that act as a critical hub like "epicenters" [71]. In the meantime, the connections between the affected hub regions and unaffected are disturbed. Thus, transregional diffusion may play an essential role in the spread of neurodegenerative pathologies during the progression of AD [72]. Current results of correlation analyses demonstrated that local connectivity abnormality of several regions is associated with interregional connectivity network properties, inferring that these regions could be the most important influencing centers in AD patients pathological progression.

In order to choose sensitive biomarkers for the discrimination of AD from CNs, complex networks of single brain regions were analyzed using fMRI data and 88.52% accuracy was achieved. In previous studies, the time series extracted from rs-fMRI images was used to establish the functional connection network with Pearson correlation coefficients between distinct brain regions, and then the random Elman neural network cluster method was used to classify AD patients from CNs, with an accuracy of 92.31% [73]. In another study, a deep autoencoder network model based on rs-fMRI data was built to categorize these correlation coefficient data and the accuracy rate was 86.47% [74]. Also, in rs-fMRI data, Wang *et al.* established frequency-dependent brain network based on the wavelet correlation, which achieved 85.7% accuracy [75]. In contrast, our proposed method has a promising future in the application of AD diagnosis.

CONCLUSION

In summary, the impaired both local complex network and functional network of abnormal IFGoperc.L, SOG.R, MOG.R, SPG.R and PCUN.R play an important role in the pathological changes of AD. We successfully classified AD data from control normal data with 88.52% accuracy using local complex network, which was constructed with the method of visibility graph. Furthermore, in the correlation analysis of the influence of local brain abnormality on global network measures, we believe that the single regional abnormality is potentially related to the disruption of interregional connections.

ETHICS APPROVAL AND CONSENT TO PARTICIPATE

The experimental procedure was approved by the Ethics Committee of General Hospital Affiliated to Tianjin Medical University, China. The reference number of the IRB approval for the study is IRB2018–038–01.

HUMAN AND ANIMAL RIGHTS

No Animals were used in this study. All humans research procedures followed were in accordance with the guidelines of the Declaration of Helsinki and Good Clinical Practice guidelines.

CONSENT FOR PUBLICATION

All participants provided written informed consent.

AVAILABILITY OF DATA AND MATERIALS

The data supporting the findings of the article is available in the Alzheimer's Disease Neuroimaging Initiative (ADNI) database at http://adni.loni.usc.edu.

FUNDING

This work was supported by National Natural Science Foundation of China Under Grant No. 61873181 and No. 61903270.

Data collection and sharing for this project was funded by the Alzheimer's Disease Neuroimaging Initiative (ADNI) (National Institutes of Health Grant U01 AG024904) and DOD ADNI (Department of Defense award number W81XWH-12-2-0012). ADNI is funded by the National Institute on Aging, the National Institute of Biomedical Imaging and Bioengineering, and through generous contributions from the following: AbbVie, Alzheimer's Association; Alzheimer's Drug Discovery Foundation; Araclon Biotech; BioClinica, Inc.; Biogen; Bristol-Myers Squibb Company; CereSpir, Inc.; Eisai Inc.; Elan Pharmaceuticals, Inc.; Eli Lilly and Company; EuroImmun; F. Hoffmann-La Roche Ltd and its affiliated company Genentech, Inc.; Fujirebio; GE Healthcare; IXICO Ltd.; Janssen Alzheimer Immunotherapy Research & Development, LLC.; Johnson & Johnson Pharmaceutical Research & Development LLC.; Lumosity; Lundbeck; Merck&Co.,Inc.;Meso Scale Diagnostics, LLC.; NeuroRx Research; Neurotrack Technologies; Novartis Pharmaceuticals Corporation; Pfizer Inc.; Piramal Imaging; Servier; Takeda Pharmaceutical Company; and Transition Therapeutics. The Canadian Institutes of Health Research is providing funds to support ADNI clinical sites in Canada. Private sector contributions are facilitated by the Foundation for the National Institutes of Health (http://www.fnih.org). The grantee organization is the Northern California Institute for Research and Education, and the study is coordinated by the Alzheimer's Disease Co-

operative Study at the University of California, San Diego. ADNI data are disseminated by the Laboratory for Neuro Imaging at the University of Southern California.

CONFLICT OF INTEREST

The authors declare no conflict of interest, financial or otherwise.

ACKNOWLEDGEMENTS

Declared none.

REFERENCES

[1] Ma C, Wang J, Zhang J, Chen K, Li X, Shu N, *et al.* Disrupted brain structural connectivity: pathological interactions between genetic apoe ε4 status and developed MCI xondition. Mol Neurobiol 54(9): 6999-7007 (2017). http://dx.doi.org/10.1007/s12035-016-0224-5 PMID: 27785756

[2] Yu H, Lei X, Song Z, Wang J, Wei X, Yu B. Functional brain connectivity in Alzheimer's disease: an EEG study based on permutation disalignment index. Physica a-Statistical Mechanics and Its ApplicationsPhysica a-Statistical Mechanics and Its Applications 506: 1093-3 (2018).

[3] Prince M, Bryce R, Albanese E, Wimo A, Ribeiro W, Ferri CP. The global prevalence of dementia: a systematic review and metaanalysis. Alzheimers Dement 9(1): 63-75.e2 (2013). http://dx.doi.org/10.1016/j.jalz.2012.11.007 PMID: 233058234

[4] McKeith IG, Galasko D, Kosaka K, Perry EK, Dickson DW, Hansen LA, *et al.* Consensus guidelines for the clinical and pathologic diagnosis of dementia with Lewy bodies (DLB): report of the consortium on DLB international workshop. Neurology 47(5): 1113-24 (1996). http://dx.doi.org/10.1212/WNL.47.5.1113 PMID: 8909416

[5] Rajasekhar K, Chakrabarti M, Govindaraju T. Function and toxicity of amyloid beta and recent therapeutic interventions targeting amyloid beta in Alzheimer's disease. Chem Commun (Camb) 51(70): 13434-50 (2015). http://dx.doi.org/10.1039/C5CC05264E PMID: 26247608

[6] Maccioni RB, Farías G, Morales I, Navarrete L. The revitalized tau hypothesis on Alzheimer's disease. Arch Med Res 41(3): 226-31 (2010). http://dx.doi.org/10.1016/j.arcmed.2010.03.007 PMID: 20682182

[7] Hardy J, Selkoe DJ. The amyloid hypothesis of Alzheimer's disease: progress and problems on the road to therapeutics. Science 297(5580): 353-6 (2002). http://dx.doi.org/10.1126/science.1072994 PMID: 12130773

[8] Yao Z, Zhang Y, Lin L, Zhou Y, Xu C, Jiang T. Alzheimer's Disease Neuroimaging Initiative. Abnormal cortical networks in mild cognitive impairment and Alzheimer's disease. PLOS Comput Biol 6(11): e1001006 (2010). http://dx.doi.org/10.1371/journal.pcbi.1001006 PMID: 21124954

[9] Seo EH, Lee DY, Lee J-M, Park J-S, Sohn BK, Lee DS, *et al.* Whole-brain functional networks in cognitively normal, mild cognitive impairment, and Alzheimer's disease. PLoS One 8(1): e53922 (2013). http://dx.doi.org/10.1371/journal.pone.0053922 PMID: 23335980

[10] Sun Y, Yin Q, Fang R, Yan X, Wang Y, Bezerianos A, *et al.* Disrupted functional brain connectivity and its association to structural connectivity in amnestic mild cognitive impairment and Alzheimer's disease. PLoS One 9(5): e96505 (2014). http://dx.doi.org/10.1371/journal.pone.0096505 PMID: 24806295

[11] Niu Y, Wang B, Zhou M, Xue J, Shapour H, Cao R, *et al.* Dynamic complexity of spontaneous BOLD activity in Alzheimer's disease and mild cognitive impairment using multiscale entropy analysis. Front Neurosci 12: 677 (2018) http://dx.doi.org/10.3389/fnins.2018.00677

[12] Wang K, Liang M, Wang L, Tian L, Zhang X, Li K, *et al.* Altered functional connectivity in early Alzheimer's disease: a resting-state fMRI study. Hum Brain Mapp 28(10): 967-78 (2007). http://dx.doi.org/10.1002/hbm.20324 PMID: 17133390

[13] Sanz-Arigita EJ, Schoonheim MM, Damoiseaux JS, Rombouts SARB, Maris E, Barkhof F, *et al.* Loss of 'small-world' networks in Alzheimer's disease: graph analysis of FMRI resting-state functional connectivity. PLoS One 5(11): e13788 (2010). http://dx.doi.org/10.1371/journal.pone.0013788 PMID: 21072180

[14] Zhang H-Y, Wang S-J, Xing J, Liu B, Ma Z-L, Yang M, *et al.* Detection of PCC functional connectivity characteristics in resting-state fMRI in mild Alzheimer's disease. Behav Brain Res 197(1): 103-8 (2009). http://dx.doi.org/10.1016/j.bbr.2008.08.012 PMID: 18786570

[15] Liu Z, Zhang Y, Yan H, Bai L, Dai R, Wei W, *et al.* Altered topological patterns of brain networks in mild cognitive impairment and Alzheimer's disease: a resting-state fMRI study. Psychiatry Res 202(2): 118-25 (2012). http://dx.doi.org/10.1016/j.pscychresns.2012.03.002 PMID: 22695315

[16] He Y, Chen Z, Evans A. Structural insights into aberrant topological patterns of large-scale cortical networks in Alzheimer's disease. J Neurosci 28(18): 4756-66 (2008). http://dx.doi.org/10.1523/JNEUROSCI.0141-08.2008 PMID: 18448652

[17] Grieder M, Wang DJJ, Dierks T, Wahlund L-O, Jann K. Default mode network complexity and cognitive decline in mild Alzheimer's disease. Frontiers in Neuroscience 12: 770 (2018). http://dx.doi.org/10.3389/fnins.2018.00770

[18] Ma C, Zhang Y, Li X, Chen Y, Zhang J, Liu Z, *et al.* The TT allele of rs405509 synergizes with APOE ε4 in the impairment of cognition and its underlying default mode network in non-demented elderly. Curr Alzheimer Res 13(6): 708-17 (2016). http://dx.doi.org/10.2174/1567205013666160129100350 PMID: 26825091

[19] Wang L, Zang Y, He Y, Liang M, Zhang X, Tian L, *et al.* Changes in hippocampal connectivity in the early stages of Alzheimer's disease: evidence from resting state fMRI. Neuroimage 31(2): 496-504 (2006). http://dx.doi.org/10.1016/j.neuroimage.2005.12.033 PMID: 16473024

[20] Buckner RL, Snyder AZ, Shannon BJ, LaRossa G, Sachs R, Fotenos AF, *et al.* Molecular, structural, and functional characterization of Alzheimer's disease: evidence for a relationship between default activity, amyloid, and memory. J Neurosci 25(34): 7709-17 (2005). http://dx.doi.org/10.1523/JNEUROSCI.2177-05.2005 PMID: 16120771

[21] Supekar K, Menon V, Rubin D, Musen M, Greicius MD. Network analysis of intrinsic functional brain connectivity in Alzheimer's disease. PLOS Comput Biol 4(6): e1000100 (2008). http://dx.doi.org/10.1371/journal.pcbi.1000100 PMID: 18584043

[22] Gao ZK, Small M, Kurths J. Complex network analysis of time series. Epl-Europhys Lett 116(5): (2016). http://dx.doi.org/10.1209/0295-5075/116/50001

[23] Gao ZK, Zhang KL, Dang WD, Yang YX, Wang ZB, Duan HB, *et al.* An adaptive optimal-Kernel time-frequency representation-based complex network method for characterizing fatigued behavior using the SSVEP-based BCI system. Knowl Base Syst 152: 163-71 (2018). http://dx.doi.org/10.1016/j.knosys.2018.04.013

[24] Gao Z, Wang X, Yang Y, Mu C, Cai Q, Dang W, *et al.* EEG-Based spatio-temporal convolutional neural network for driver fatigue evaluation. IEEE Trans Neural Netw Learn Syst 30(9): 2755-63 (2019). http://dx.doi.org/10.1109/TNNLS.2018.2886414 PMID: 30640634

[25] Lacasa L, Luque B, Ballesteros F, Luque J, Nuño JC. From time series to complex networks: the visibility graph. Proc Natl Acad Sci USA 105(13): 4972-5 (2008). http://dx.doi.org/10.1073/pnas.0709247105 PMID: 18362361

[26] Yu M, Hillebrand A, Gouw AA, Stam CJ. Horizontal visibility graph transfer entropy (HVG-TE): a novel metric to characterize directed connectivity in large-scale brain networks. Neuroimage 156: 249-64 (2017). http://dx.doi.org/10.1016/j.neuroimage.2017.05.047 PMID: 28539247

[27] Ahmadlou M, Adeli H, Adeli A. Improved visibility graph fractality with application for the diagnosis of Autism Spectrum

Disorder. Physica a-Statistical Mechanics and Its Applications 391(20): 4720-26 (2012).
http://dx.doi.org/10.1016/j.physa.2012.04.025

[28] Gao ZK, Cai Q, Yang YX, Dong N, Zhang SS. Visibility graph from adaptive optimal kernel time-frequency representation for classification of epileptiform EEG. Int J Neural Syst 27(4): 1750005 (2017).
http://dx.doi.org/10.1142/S0129065717500058 PMID: 27832712

[29] Cai Q, Gao ZK, Yang YX, Dang WD, Grebogi C. Multiplex Limited Penetrable Horizontal Visibility Graph from EEG Signals for Driver Fatigue Detection. Int J Neural Syst 29(5): 1850057 (2019).
http://dx.doi.org/10.1142/S0129065718500570 PMID: 30776986

[30] Ahmadlou M, Adeli H, Adeli A. New diagnostic EEG markers of the Alzheimer's disease using visibility graph. J Neural Transm (Vienna) 117(9): 1099-109 (2010).
http://dx.doi.org/10.1007/s00702-010-0450-3 PMID: 20714909

[31] Bullmore E, Sporns O. Complex brain networks: graph theoretical analysis of structural and functional systems. Nat Rev Neurosci 10(3): 186-98 (2009).
http://dx.doi.org/10.1038/nrn2575 PMID: 19190637

[32] Dai Z, Yan C, Li K, Wang Z, Wang J, Cao M, *et al.* Identifying and mapping connectivity patterns of brain network hubs in Alzheimer's disease. Cereb Cortex 25(10): 3723-42 (2015).
http://dx.doi.org/10.1093/cercor/bhu246 PMID: 25331602

[33] Lacasa L, Luque B, Luque J, Nuno JC. The visibility graph: a new method for estimating the Hurst exponent of fractional Brownian motion. Epl-Europhys Lett 86(3): (2009).
http://dx.doi.org/10.1209/0295-5075/86/30001

[34] Rubinov M, Sporns O. Complex network measures of brain connectivity: uses and interpretations. Neuroimage 52(3): 1059-69 (2010).
http://dx.doi.org/10.1016/j.neuroimage.2009.10.003 PMID: 19819337

[35] Goel K, Singh RR, Iyengar S, Gupta S. A faster algorithm to update betweenness centrality after node alteration. Internet Math 11(4-5): 403-20 (2015).
http://dx.doi.org/10.1080/15427951.2014.982311

[36] Chang P, Li X, Ma C, Zhang S, Liu Z, Chen K, *et al.* The effects of an APOE promoter polymorphism on human white matter connectivity during non-demented aging. J Alzheimers Dis 55(1): 77-87 (2017).
http://dx.doi.org/10.3233/JAD-160447 PMID: 27636845

[37] Opsahl T. Triadic closure in two-mode networks: redefining the global and local clustering coefficients. Soc Networks 35(2): 159-67 (2013).
http://dx.doi.org/10.1016/j.socnet.2011.07.001

[38] Feng X, Zhao Y, Zhang C, Cheng P, He Y. Discrimination of transgenic maize kernel using NIR hyperspectral imaging and multivariate data analysis. Sensors (Basel) 17(8): E1894 (2017).
http://dx.doi.org/10.3390/s17081894 PMID: 28817075

[39] Wang S, Liu S, Che X, Wang Z, Zhang J, Kong D. Recognition of polycyclic aromatic hydrocarbons using fluorescence spectrometry combined with bird swarm algorithm optimization support vector machine. Spectrochimica Acta Part a-Molecular and Biomolecular Spectroscopy 22(4): (2020)
http://dx.doi.org/10.1016/j.saa.2019.117404

[40] Dai S, Niu D, Han Y. Forecasting of Power grid investment in china based on support vector machine optimized by differential evolution algorithm and grey wolf optimization algorithm applied sciences-basel 84 (2018).
http://dx.doi.org/10.3390/app8040636

[41] Cervantes J, Garcia-Lamont F, Rodriguez-Mazahua L, Lopez A, Ruiz-Castilla J, Trueba A. PSO-based method for SVM classification on skewed data sets. Neurocomputing 228: 187-97 (2017).
http://dx.doi.org/10.1016/j.neucom.2016.10.041

[42] Chang C-C, Lin C-J. LIBSVM: A Library for Support Vector Machines. ACM Trans Intell Syst Technol 2(3): (2011).
http://dx.doi.org/10.1145/1961189.1961199

[43] Wang J, Yang C, Wang RF, Yu HT, Cao YB, Liu J. Functional brain networks in Alzheimer's disease: EEG analysis based on limited penetrable visibility graph and phase space method. Physica a-Statistical Mechanics App 460: 174-87 (2016).

[44] Naqvi NH, Rudrauf D, Damasio H, Bechara A. Damage to the insula disrupts addiction to cigarette smoking. Science 315(5811): 531-4 (2007).
http://dx.doi.org/10.1126/science.1135926 PMID: 17255515

[45] Kurth F, Zilles K, Fox PT, Laird AR, Eickhoff SB. A link between the systems: functional differentiation and integration within the human insula revealed by meta-analysis. Brain Struct Funct 214(5-6): 519-34 (2010).
http://dx.doi.org/10.1007/s00429-010-0255-z PMID: 20512376

[46] Zhao Z-L, Fan F-M, Lu J, Li H-J, Jia L-F, Han Y, *et al.* Changes of gray matter volume and amplitude of low-frequency oscillations in amnestic MCI: An integrative multi-modal MRI study. Acta Radiol 56(5): 614-21 (2015).
http://dx.doi.org/10.1177/0284185114533329 PMID: 24792358

[47] Karas GB, Scheltens P, Rombouts SA, Visser PJ, van Schijndel RA, Fox NC, *et al.* Global and local gray matter loss in mild cognitive impairment and Alzheimer's disease. Neuroimage 23(2): 708-16 (2004).
http://dx.doi.org/10.1016/j.neuroimage.2004.07.006 PMID: 15488420

[48] Braak H, Alafuzoff I, Arzberger T, Kretzschmar H, Del Tredici K. Staging of Alzheimer disease-associated neurofibrillary pathology using paraffin sections and immunocytochemistry. Acta Neuropathol 112(4): 389-404(2006).
http://dx.doi.org/10.1007/s00401-006-0127-z PMID: 16906426

[49] He W, Liu D, Radua J, Li G, Han B, Sun Z. Meta-analytic comparison between PIB-PET and FDG-PET results in Alzheimer's disease and MCI. Cell Biochem Biophys 71(1): 17-26 (2015).
http://dx.doi.org/10.1007/s12013-014-0138-7 PMID: 25370296

[50] Xie C, Bai F, Yu H, Shi Y, Yuan Y, Chen G, *et al.* Abnormal insula functional network is associated with episodic memory decline in amnestic mild cognitive impairment. Neuroimage 63(1): 320-7 (2012).
http://dx.doi.org/10.1016/j.neuroimage.2012.06.062 PMID: 22776459

[51] Seeley WW, Menon V, Schatzberg AF, Keller J, Glover GH, Kenna H *et al.* Dissociable intrinsic connectivity networks for salience processing and executive control. J Neurosci 27(9): 2349-56 (2007).
http://dx.doi.org/10.1523/JNEUROSCI.5587-06.2007 PMID: 17329432

[52] Li H, Jia X, Qi Z, Fan X, Ma T, Ni H, *et al.* Altered functional connectivity of the basal nucleus of meynert in mild cognitive impairment: a resting-state FMRI Study. Front Aging Neurosci 9: 127 (2017).

[53] Mesulam MM, Volicer L, Marquis JK, Mufson EJ, Green RC. Systematic regional differences in the cholinergic innervation of the primate cerebral cortex: distribution of enzyme activities and some behavioral implications. Ann Neurol 19(2): 144-51 (1986).
http://dx.doi.org/10.1002/ana.410190206 PMID: 3963756

[54] Maddock RJ. The retrosplenial cortex and emotion: new insights from functional neuroimaging of the human brain. Trends Neurosci 22(7): 310-6 (1999).
http://dx.doi.org/10.1016/S0166-2236(98)01374-5 PMID: 10370255

[55] Xu L, Wu X, Li R, Chen KW, Long ZY, Zhang JC, *et al.* Alzheimer's disease neuroimaging initiative. Prediction of progressive mild cognitive impairment by multi-modal neuroimaging biomarkers. J Alzheimers Dis 51(4): 1045-56 (2016).
http://dx.doi.org/10.3233/JAD-151010 PMID: 26923024

[56] Camus V, Payoux P, Barré L, Desgranges B, Voisin T, Tauber C, *et al.* Using PET with 18F-AV-45 (florbetapir) to quantify brain amyloid load in a clinical environment. Eur J Nucl Med Mol Imaging 39(4): 621-31(2012).
http://dx.doi.org/10.1007/s00259-011-2021-8 PMID: 22252372

[57] Farrow TFD, Thiyagesh SN, Wilkinson ID, Parks RW, Ingram L, Woodruff PWR. Fronto-temporal-lobe atrophy in early-stage Alzheimer's disease identified using an improved detection methodology. Psychiatry Res 155(1): 11-9 (2007).
http://dx.doi.org/10.1016/j.pscychresns.2006.12.013 PMID: 17399959

[58] Ting WK-C, Fischer CE, Millikin CP, Ismail Z, Chow TW, Schweizer TA. Grey matter atrophy in mild cognitive impairment /

early Alzheimer disease associated with delusions: a voxel-based morphometry study. Curr Alzheimer Res 12(2): 165-72 (2015). http://dx.doi.org/10.2174/1567205012666150204130456 PMID: 25654501

[59] Mazoyer B, Zago L, Mellet E, Bricogne S, Etard O, Houde O, *et al.* Cortical networks for working memory and executive functions sustain the conscious resting state in man. Brain Res Bull 54(3): 287-98 (2001). http://dx.doi.org/10.1016/S0361-9230(00)00437-8 PMID: 11287133

[60] McKiernan KA, Kaufman JN, Kucera-Thompson J, Binder JR. A parametric manipulation of factors affecting task-induced deactivation in functional neuroimaging. J Cogn Neurosci 15(3): 394-408 (2003). http://dx.doi.org/10.1162/089892903321593117 PMID: 12729491

[61] Greicius MD, Menon V. Default-mode activity during a passive sensory task: uncoupled from deactivation but impacting activation. J Cogn Neurosci 16(9): 1484-92 (2004). http://dx.doi.org/10.1162/0898929042568532 PMID: 15601513

[62] Duarte-Abritta B, Villarreal MF, Abulafia C, *et al.* Cortical thickness, brain metabolic activity, and in vivo amyloid deposition in asymptomatic, middle-aged offspring of patients with late-onset Alzheimer's disease. J Psychiatr Res 107: 11-8 (2018). http://dx.doi.org/10.1016/j.jpsychires.2018.10.008 PMID: 30308328

[63] Binnewijzend MAA, Adriaanse SM, Van der Flier WM, *et al.* Brain network alterations in Alzheimer's disease measured by eigenvector centrality in fMRI are related to cognition and CSF biomarkers. Hum Brain Mapp 35(5): 2383-93 (2014). http://dx.doi.org/10.1002/hbm.22335 PMID: 24039033

[64] Wang Z, Jia X, Liang P, Qi Z, Yang Y, Zhou W, *et al.* Changes in thalamus connectivity in mild cognitive impairment: evidence from resting state fMRI. Eur J Radiol 81(2): 277-85 (2012). http://dx.doi.org/10.1016/j.ejrad.2010.12.044 PMID: 21273022

[65] Holroyd S, Shepherd ML, Downs JH III. Occipital atrophy is associated with visual hallucinations in Alzheimer's disease. J Neuropsychiatry Clin Neurosci 12(1): 25-8 (2000). http://dx.doi.org/10.1176/jnp.12.1.25 PMID: 10678508

[66] Wang B, Niu Y, Miao L, Cao R, Yan P, Guo H, *et al.* Decreased Complexity in Alzheimer's Disease: Resting-State fMRI Evidence of Brain Entropy Mapping. Frontiers Aging Neurosci 9: 378 (2017).

[67] Zheng W, Yao Z, Hu B, Gao X, Cai H, Moore P. Novel cortical thickness pattern for accurate detection of Alzheimer's disease. J Alzheimers Dis 48(4): 995-1008 (2015). http://dx.doi.org/10.3233/JAD-150311 PMID: 26444768

[68] Chételat G, Landeau B, Eustache F, enge F, Viader F, de la Sayette V, et *et al.* Using voxel-based morphometry to map the structural changes associated with rapid conversion in MCI: a longitudinal MRI study. Neuroimage 27(4): 934-46 (2005). http://dx.doi.org/10.1016/j.neuroimage.2005.05.015 PMID: 15979341

[69] Cavanna AE, Trimble MR. The precuneus: a review of its functional anatomy and behavioural correlates. Brain 129(Pt 3): 564-83 (2006). http://dx.doi.org/10.1093/brain/awl004 PMID: 16399806

[70] Delbeuck X. Van dL, M, Collette FJNR. Alzheimer'. Disease as a Disconnection Syndrome 13(2): 79-92 (2003).

[71] Zhou J, Gennatas ED, Kramer JH, Miller BL, Seeley WW. Predicting regional neurodegeneration from the healthy brain functional connectome. Neuron 73(6): 1216-27 (2012). http://dx.doi.org/10.1016/j.neuron.2012.03.004 PMID: 22445348

[72] Raj A, Kuceyeski A, Weiner M. A network diffusion model of disease progression in dementia. Neuron 73(6): 1204-15 (2012). http://dx.doi.org/10.1016/j.neuron.2011.12.040 PMID: 22445347

[73] Bi X-a, Jiang Q, Sun Q, Shu Q, Liu Y. Analysis of Alzheimer's disease based on the random neural network cluster in FMRI. Front Neuroinform 12: 60 (2018). http://dx.doi.org/10.3389/fninf.2018.00060

[74] Ju R, Hu C, Zhou P, Li Q. Early diagnosis of Alzheimer's disease based on resting-state brain networks and deep learning. IEEE/ACM Trans Comput Biol Bioinformatics 16(1): 244-57 (2019). http://dx.doi.org/10.1109/TCBB.2017.2776910 PMID: 29989989

[75] Wang J, Zuo X, Dai Z, Xia M, Zhao Z, Zhao X, *et al*. Disrupted functional brain connectome in individuals at risk for Alzheimer's disease. Biol Psychiatry 73(5): 472-81 (2013). http://dx.doi.org/10.1016/j.biopsych.2012.03.026 PMID: 22537793